Journal of Cancer Research and Clinical Oncology (2019) 145:1405–1416
https://doi.org/10.1007/s00432-019-02901-7

ORIGINAL ARTICLE – CANCER RESEARCH

NOD1 and NOD2 of the innate immune system is differently expressed in human clear cell renal cell carcinoma, corresponding healthy renal tissue, its vasculature and primary isolated renal tubular epithelial cells

Lilli Mey[1] · Michaela Jung[2] · Frederik Roos[3] · Roman Blaheta[3] · Axel Hegele[4] · Ralf Kinscherf[1] · Anja Urbschat[4,5]

Received: 22 October 2018 / Accepted: 19 March 2019 / Published online: 22 March 2019

Abstract

Purpose NOD1 and NOD2 (nucleotide-binding oligomerization domain)—receptors are intracellular receptors and belong to the family of pattern recognition receptors being present in both human and murine renal tubular cells. Besides, NOD1 has been proved to promote apoptosis, upon its overexpression. Hence, we aimed to investigate NOD1 and NOD2 expression in human clear cell renal cell carcinoma (ccRCC).

Methods Tumor and corresponding adjacent healthy tissues from 41 patients with histopathological diagnosis of ccRCC as well as primary isolated renal tubular epithelial cells (TECs) and tumor tissue from a murine xenograft model using CAKI-1 ccRCC cells were analyzed.

Results NOD1 and NOD2 mRNA was constitutively expressed in both tumor and adjacent healthy renal tissue, with NOD1 being significantly lower and in contrast NOD2 significantly higher expressed in tumor tissue compared to healthy tissues. Immunohistochemically, NOD1 was located not only in the cytoplasm, but also in the nucleus in ccRCC tissue whereas NOD2 was solely localized in the cytoplasm in both human ccRCC as well as in the healthy tubular system. Focusing on the vasculature, NOD2 displayed broader expression than NOD1. In primary TECs as well as CAKI-1 cells NOD1 and NOD2 was constitutively expressed and increasable upon LPS stimulation. In the mouse xenograft model, human NOD1 mRNA was significantly higher expressed compared to NOD2. In contrast hereto, we observed a shift towards lower mouse NOD1 compared to NOD2 mRNA expression.

Conclusion In view of reduced apoptosis-associated NOD1 expression in ccRCC tissue opposed to higher expression of NOD2 in tumor vasculature, inducibility of NOD expression in TECs as well as the detected shift of NOD1 and NOD2 expression in the mouse xenograft model, modulation of NOD receptors might, therefore, provide a molecular therapeutic approach in ccRCC.

Keywords Kidney cancer · Clear cell renal cell carcinoma · Innate immunity · NLR

Electronic supplementary material The online version of this article (https://doi.org/10.1007/s00432-019-02901-7) contains supplementary material, which is available to authorized users.

✉ Anja Urbschat
anja.urbschat@biomed.au.dk

[1] Department of Medical Cell Biology, Institute for Anatomy and Cell Biology, Philipps-University of Marburg, Marburg, Germany

[2] Institute of Biochemistry I, Goethe-University Frankfurt, Frankfurt am Main, Germany

[3] Clinic of Urology, Goethe-University Frankfurt, Frankfurt am Main, Germany

[4] Clinic of Urology and Pediatric Urology, Philipps-University Marburg, Marburg, Germany

[5] Department of Biomedicine, Aarhus University, Bartholins Allé 6, 8000 Aarhus C, Denmark

Introduction

Renal cell carcinoma (RCC) occurs worldwide with about 403,262 new cases yearly (Bray et al. 2018). Hereof, clear cell renal cell carcinoma (ccRCC) is the most frequently diagnosed histological entity with about 80% of cases (Patard et al. 2005). Since renal cell carcinoma is hardly sensitive to chemo- or radio-therapy, both unspecific immune- and targeted-therapy as well as recently immune checkpoint inhibitors represent the standard treatment in metastasized RCC (Bamias et al. 2017). In this context, great attention is paid to the capacity of immunity to control cancer (Koebel et al. 2007). It is known that the immune system affects and shapes tumor growth through close communication between immune and malignant cells. With regard to immunotherapy, members of the toll-like receptor family (TLRs) of the innate immune system have been extensively investigated in oncogenesis (Braunstein et al. 2018). Additionally, a second protein family has been discovered: The NLR/NOD/Caterpillar family, which is equally attributed to the innate immune system (Ting and Davis 2005).

NOD (nucleotide-binding oligomerization domain)-like receptors are intracellular receptors which belong to the family of pattern recognition receptors (PRRs) (Caruso et al. 2014). Hereof, NOD1 (Caspase Recruitment Domain 4; CARD4) and NOD2 (CARD15) were first described as intracellular receptors for bacterial lipopolysaccharide (LPS) (Inohara et al. 2001). Moreover, NOD2 reveals structural and functional similarity to NOD1 (Ogura et al. 2001) and both possess binding sites for ligands, a central NOD, and a N-terminal caspase recruitment domain (CARD) that binds the downstream signaling molecule RICK (also called RIP2 or CARDIAK), a protein kinase that activates NF-kB (Bertin et al. 1999; Inohara et al. 2001).

NOD1 is widely expressed in a variety of cell types, such as epithelial, mesothelial, and endothelial cells (Inohara et al. 1999; Park et al. 2007). In contrast, NOD2 expression seems to be limited to leukocytes (Ogura et al. 2001) and specified epithelial cell types, like intestinal (Ogura et al. 2003) or renal tubular epithelial cells (Shigeoka et al. 2010) as well as vascular endothelial cells (Oh et al. 2005; Davey et al. 2006).

Focusing on the kidney, human kidney epithelial cells in culture constitutively express both NOD1 and NOD2 being intracellularly localized (Uehara et al. 2007). Besides, NOD1 and NOD2 are equally present in murine renal tubular cells and their deficiency provides protection in renal ischemia reperfusion injury, mainly in terms of reduced apoptosis (Shigeoka et al. 2010). Both seem to play an important role in the pathogenesis of acute ischemic kidney injury, although possibly through different mechanisms (Shigeoka et al. 2010). Further investigations during systemic inflammation in NOD1 and NOD2 knock-out mice affirmed a significant renal tissue-specific signal transduction by NOD1 and NOD2 (Stroo et al. 2012). Furthermore, NOD1 mRNA has been investigated in embryonic development, and although NOD1 labeling exhibited a rather restricted distribution in embryonic tissues, it was also detectable in the cortical region of the embryonic kidney (Inohara et al. 1999). Thus, NOD1, and potentially also NOD2, seem to be important during both development and pathological settings of tissue injury of the renal tubular system. This is insofar of interest, as ccRCC derives from the renal tubular system (Thoenes et al. 1986).

Therefore, in the present study, we investigated the expression and immuno-histological localization of NOD1 and NOD2 in human ccRCC tissue, adjacent healthy renal tissue, primary isolated renal tubular epithelial cells (TECs) from ccRCC and healthy renal tissue as well as in a mouse xenograft tumor model employing CAKI-1 cells.

Materials and methods

Participants

The study protocol and consent documents were approved by the local Ethic Committee of the Goethe-University Hospital Frankfurt am Main (file number 04/09 UGO 03/10) and Philipps-University Hospital Marburg (file number 122/14). Patients gave their informed consent prior to surgery. Tumor and corresponding adjacent healthy tissues were obtained from 41 patients with histopathological diagnosis of ccRCC. Clinical characteristics of these patients are listed in Table 1. Patient exclusion criteria comprised immunodeficiency, autoimmune diseases or second malignancy to eliminate factors interfering with the measurements. All patients underwent imaging (CT and/or MRI) for preoperative staging and

Table 1 Characteristics of the study population

Parameter	
Number of patients	41
Mean age Median age	64 63
Age x–x	42–84
Female	34%
Male	66%
pT1/2	54%
pT3/4	46%
G1/2	83%
G3/4	17%

surgery before receiving any other therapy. Specimens of the tumor tissue as well as adjacent healthy renal tissues were collected from each patient immediately after radical nephrectomy. Samples were fresh frozen or have been paraffin embedded after fixation until further processing. The pathological examination was performed according to the actual UICC TNM classification of malignant tumors.

Xenograft model and cell culture

Male 3–4 weeks old NMRI-Foxn1nu/Foxn1nu (Janvier, France) were kept in the central research facility of the University-Hospital Frankfurt. They were housed with water and food ad libitum in rooms with a 12-h light cycle. The procedures involving animals were approved by the Animal Care and Use Committee of the state of Hesse, Germany (V54-19c 20/15-F35/06). Surgery and animal care were performed in accordance with the "Guide for the care and use of laboratory animals" (National Institutes of Health, volume 25, no. 28, revised 1996), EU Directive 86/609 EEC and German Protection of Animals Act. The human ccRCC cell lines CAKI-1 was cultured in Dulbecco's modified Eagle's medium (DMEM; Gibco, 41965) with high glucose, supplemented with 10% FCS and 1% penicillin/streptomycin. We performed a xenograft model by applying 1.5×10^7 CAKI-1 (ccRCC cell line) in 100 µl sterile PBS subcutaneously in the flank. Animals were scored for tumor formation every second day and sacrificed after 14 days. Complete tumors were carefully removed, and divided longitudinally into halves. One-half was placed in 4% paraformaldehyde overnight, the other half was stored at − 80 °C until further processing.

Gene expression analysis by real-time quantitative reverse transcription-PCR

Total RNA from human tissue samples was isolated using tri-reagent (Sigma-Aldrich) and integrity was assessed on a denaturing agarose gel stained with ethidium bromide (Supp Fig. 1B). Intact RNA was transcribed using random hexameric primers and reverse transcriptase (Applied Biosystems). The following TaqMan sondes were employed: RPL-PO: Hs99999902_m1, NOD1: Hs00196075_m1, NOD2: Hs00223394_m1 (LifeTechnologies). Taq Man Fast Advanced Master Mix (Applied Biosystems) was used as Assay Mix. Realtime-PCR was performed on AbiPrism 7500 Fast Sequence Detector (Applied Biosystems). Calculation of threshold cycles (Ct values) and data analyses were performed by the sequence detector software. Total RNA from murine tumors was isolated from homogenized tissue ($n = 6$) using tri reagent (Sigma-Aldrich) according to the manufacturer's protocol. cDNA was synthesized using an iScript cDNA Synthesis kit (Bio-Rad laboratories, Hercules, USA). Gene expression profiles from all samples were assessed in duplicates by Realtime-PCR using a StepOne Plus Realtime-PCR device (Applied Biosystems, USA), applying the following primer sequences: m/h18s forw: GTAACCCGT TGAACCCCATT and rev: CCATCCAATCGGTAGTAG CG, mNOD1 forw: ACCCCATTGGGTTGTCACTC and rev: TTCGGCTGAGAAGTAGCCATT, mNOD2 forw: TGG ACACAGTCTGGAACAAGG and rev: CAGGACCATACA GTTCAAAGG, hNOD1 forw: AGTGAAAAGCAATCG GGAACTT and rev: CACACACATCTCCGCATT, hNOD2 forw: ATGGGCTTTGATGGGGGAAG and rev: AGCACA TTTCACAAGCCGGA. Relative changes in mRNA expression were calculated by normalizing the values to their corresponding RPL-PO or 18 s expression, respectively, using the 2^{-dCt} method (Livak and Schmittgen 2001).

Protein isolation and western blot analysis

For detection of intracellular proteins, a lysis buffer supplemented with protease inhibitor was added to human tissue samples. The extracts were clarified by centrifugation and stored at − 80 °C until use. Total protein concentrations of tissue homogenates were determined by the method according to Bradford. For western blotting, 50 µg of total protein were used per lane. Membranes were incubated with NOD1 antibody (MBS9210162, MyBioSource, dilution 1:500), NOD2 antibody (NB100-524, Novus Biologicals; dilution 1:500), and β-actin (#sc-47778, Santa Cruz, dilution 1:1000) followed by incubation with the corresponding IRDye®800 secondary antibody (926-32213 or 926-32212, LI-COR, dilution 1:10,000). Relative protein expression of NOD1 (110 kDa) and NOD2 (110 kDa) was calculated by normalizing the values to their corresponding β-actin (43 kDa) expression. Western Blots were visualized using an Odyssey™ Infrared Imaging System and protein densitometry was determined using ImageJ.

Flow cytometric analysis of NOD1 and NOD2

Patient tissue was dissociated using the human Tumor Dissociation Kit (Miltenyi, 130-095-929) and the GentleMACS system (Miltenyi). Sample acquisition was done on a LSRII/Fortessa flow cytometer (BD) expressed as mean fluorescence intensity (MFI). Both antibodies and secondary reagents were titrated to determine optimal concentrations. CompBeads (BD) were used for single color compensation to create multi-color compensation matrices. For gating, fluorescence minus one (FMO) controls were used. Cytometer setup and tracking beads (BD) were used for daily control of instrument calibration. NOD1 (MBS9210162, MyBioSource, dilution 1:100) and NOD2 (Novus Biologicals, NB 100-524, dilution 1:100) was stained intracellularly in combination with an AF546-labeled secondary antibody,

respectively (Life technologies, A-11035), after fixation and permeabilization with Cytofix/Cytoperm (BD, 554714).

Isolation and culture of primary human tubular epithelial cells (TECs) from tumor tissue and adjacent healthy renal tissue

Human primary tubular epithelial cells (TECs) were isolated from ccRCC and corresponding healthy renal tissue from two patients undergoing tumor nephrectomies as previously described (Baer et al. 1997). The procurement procedure was approved by the ethics committee of the Goethe-University Frankfurt, Germany, file number UGO 03/10–4/09 and by the ethics committee of the Philipps-University, Marburg, Germany, file number: AZ 122714. For TEC isolation, the tissue was minced and digested with collagenase and dispase. The digested fragments were passed through a 125-µm mesh and incubated with collagenase IV, DNAse and $MgCl_2$. After Percoll density gradient centrifugation cells were grown in medium 199 (# 4530, Sigma-Aldrich) supplemented with 10% FCS and 1% penicillin/streptomycin at 37 °C and 5% CO_2 in a humidified atmosphere. TECs used for the experiments were in passage 3–5 and seeded in chamber slides for immunohistochemical staining.

Immunohistochemical and immunofluorescence staining

After deparaffinization 5-µm sections, slides from ccRCC specimens, healthy adjacent renal tissue, heterotopic mouse tumor, human and murine ileum were incubated with heated 10 nM sodium citrate buffer (pH 6.0). TECs and CAKI-1 cells cultivated in chamber slides were fixed in ice-cold Aceton/Methanol. For immunohistochemistry, specimens were washed with peroxide buffer (3% in phosphate buffer) and afterwards blocked with goat serum. Polyclonal rabbit anti-human NOD1 (MBS9210162, MyBioSource, dilution 1:50), rabbit anti-human NOD2 (sc-30199, Santa Cruz, dilution 1:100), and monoclonal mouse anti-human CD13 (301702, Biolegend, dilution 1:100) were used for incubation of tissue sections overnight at 4 °C. A polyclonal goat anti rabbit–horse radish peroxidase coupled antibody (ZRH1158, Linaris, dilution 1:200), DAB substrate (11718096001, Roche) and Mayer's haemalum were used for immunohistochemical staining procedure and goat anti rabbit-Cy3 (111-165-003, Dianova, dilution 1:200), goat and mouse-Alexa 488 (ab150113, abcam, dilution 1:200) as well as DAPI (D9542, Sigma, 1 µg/ml) were used for immunofluorescence staining. Negative controls were conducted with PBS instead of primary antibody. Slides were assessed with either Zeiss AxioImager M2 microscope or confocal microscopy (Nikon, Eclipse Ti).

Nuclear localization sequences

To predict the possible existence of nuclear localization sequences, the cNLS Mapper open software (http://nls-mapper.iab.keio.ac.jp/cgi-bin/NLS_Mapper_form.cgi) was applied. This program is based on Kosugi et al. (Kosugi et al. 2009).

Statistical analyses

Statistical analyses were performed applying GraphPad Prism® 5.02 software (GraphPad Software, Inc). The distribution of variables was tested for normality using the Kolmogorov–Smirnov test. Accordingly, statistical significance was calculated using the Wilcoxon matched pairs test for paired analysis of tumor and adjacent healthy tissue. The Mann Whitney test was used for unpaired analysis in sex differences. The *t* test was used for unpaired analysis of mouse xenograft data. Significance of correlations was determined by Spearman's test including all investigated groups. p values ≤ 0.05 were assumed as statistically significant. In Fig. 1, horizontal lines within the boxes represent medians; boxes represent the interquartile range (25–75%). Whiskers above and below the box indicate the 90th and 10th percentiles. The individual points that are plotted beyond the whiskers represent outliers, which were included in the statistical analyses. In Fig. 6, horizontal lines within the boxes represent means and SEM.

Results

Inverse regulation of NOD1 and NOD2 mRNA in human ccRCC tissue compared to adjacent healthy renal tissue

Messenger RNA expression of NOD1 and NOD2 normalized to its RPL-PO content was detectable in both tumor and adjacent healthy tissue. NOD1 mRNA expression was significantly lower expressed in human tumor tissue compared to adjacent healthy tissue ($n=41$, $p<0.001$) (Fig. 1a). In contrast, NOD2 mRNA expression was significantly enhanced in tumor tissue as compared to adjacent healthy tissue ($n=41$, $p<0.01$) (Fig. 1a). Interestingly, individual NOD1 mRNA expression in tumor tissue correlated with its expression in healthy tissue ($n=41$, Spearman $r=0.4568$; $p<0.01$) (Fig. 1b) as well as individual NOD2 mRNA of these patients ($n=41$, Spearman $r=0.3622$; $p<0.5$) (Fig. 1b). Female subjects displayed a significantly higher NOD1 mRNA level in healthy renal tissue compared to male subjects ($p<0.05$), but not in tumor tissue (ns) (Fig. 1d) while NOD2 mRNA did not display differences (figure not shown). However, NOD1 and NOD2 protein levels remained

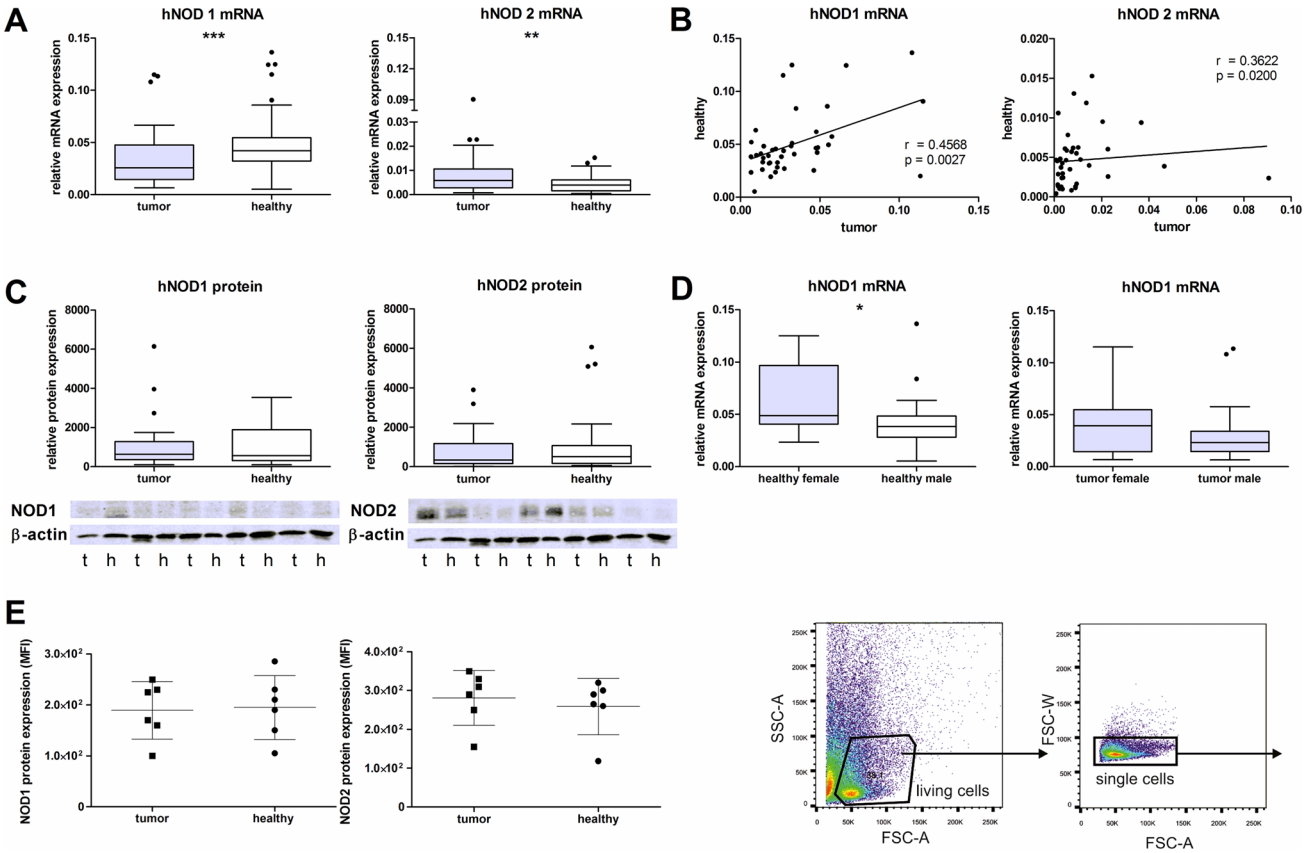

Fig. 1 mRNA and protein expression in ccRCC and healthy human kidney tissue. **a** NOD1 and NOD2 mRNA expression normalized to its RPL-PO content in tumor and adjacent healthy renal tissue ($n=33$) **b** and their correlation ($n=33$) (Spearman's rank correlation test). **d** NOD1 mRNA in female and male subjects. **c** Protein expression of NOD1 (110 kDa), NOD2 (110 kDa) and β-actin (43 kDa) ($n=23$) with representative western blots. **e** Mean fluorescence intensity in flow cytometric analysis of intracellular NOD1 and NOD2 ($n=6$). NOD mRNA and protein expression are represented in box blots to depict the distributions of the relative expression values. $*p<0.5$, $**p<0.01$, $***p<0.001$

unaltered in tumor and healthy tissue ($n=23$; ns) (Fig. 1c). The same applied for flow cytometric analysis of intracellular NOD1 and NOD2 ($n=6$) (Fig. 1e).

Distinct localization of NOD1 and NOD2 in human renal cell carcinoma tissue compared to adjacent healthy renal tissue and its respective vasculature

We further analyzed the localization of NOD1 and NOD2 in human ccRCC as well as in adjacent healthy renal tissue by immunohistochemistry (Fig. 2) and immunofluorescence (Fig. 3). The latter to co-localize NOD1 or NOD2 with CD13 as a marker for the proximal tubule. Additionally, mucosa of human and murine ileum was used as a positive control with generally known high expression of NOD1 and NOD2 (Hisamatsu et al. 2003; Ogura et al. 2003; Parlato and Yeretssian 2014). Interestingly, NOD1 was located in the cytoplasm as well as in the nucleus in both ccRCC and healthy renal tissue. In contrast, NOD2 was solely localized in the cytoplasm in both human ccRCC as well as in the tubular system of adjacent healthy renal tissue. Immunofluorescence staining confirmed higher NOD1 expression in healthy renal tissue, especially in the proximal tubule, distal tubule, and collecting duct compared to ccRCC tissue. As NOD1 and NOD2 are known to be expressed in human endothelial cells (Oh et al. 2005; Opitz et al. 2005; Davey et al. 2006) we further examined the vasculature within tumor and healthy renal tissues. Within the vasculature NOD1 or NOD2 were localized in endothelial cells of the tunica intima and smooth muscle cells of the tunica media. Hereof, NOD2 displayed higher and broader expression within the vasculature than NOD1 (Fig. 4).

Analysis of the sequences of NOD1 and NOD2 applying the publically available cNLS Mapper software, substantiated the above explained observation of NOD1 and NOD2 localization. Only NOD1 showed the nuclear localization sequence "LRRKRKALW" with a very high score of 9. However, no predicted nuclear localization sequence was

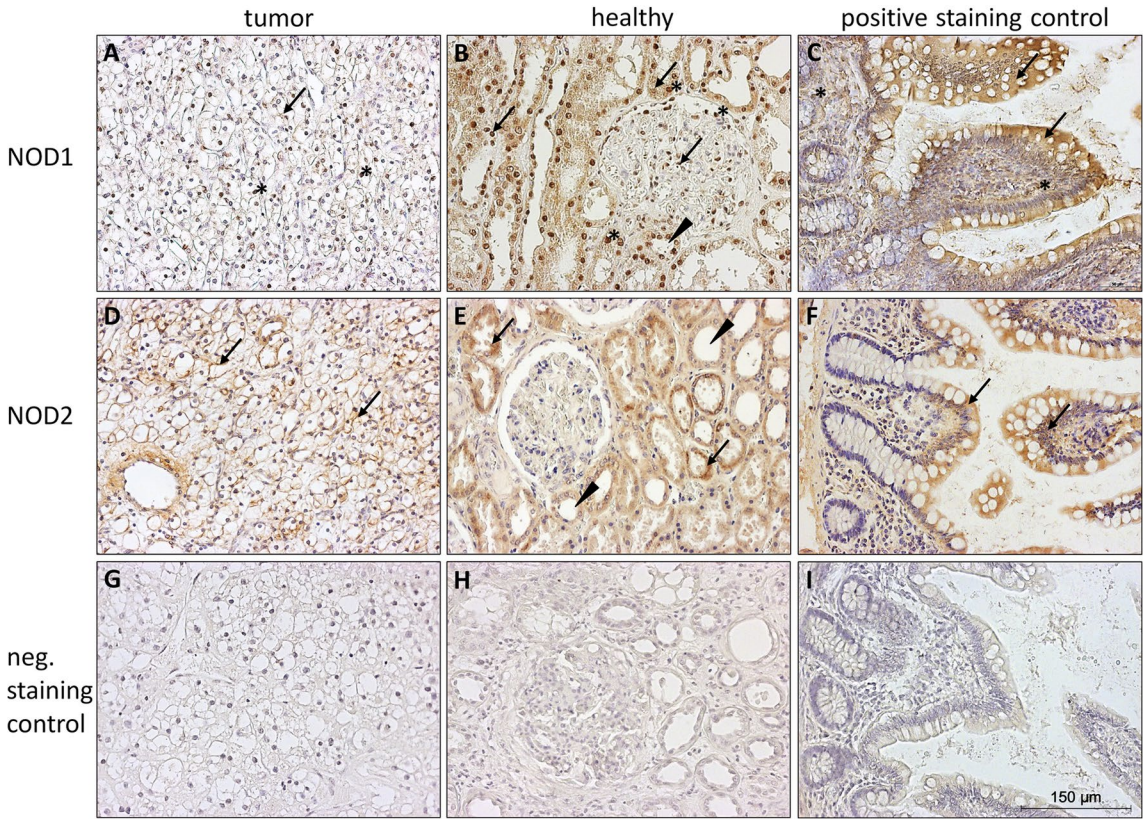

Fig. 2 Immunohistochemical staining for NOD1 and NOD2 receptors in ccRCC and healthy human kidney tissue. **a** Localization of NOD1 in the cytoplasm (arrows) and nucleus (*) of ccRCC cells. **b** Arrows indicate localization of NOD1 receptor in the cytoplasm and nucleus (*) of the tubular system, podocytes and vascular cells in healthy kidney. Arrowhead indicates a tubule. **c** High expression of NOD1 receptor in the lamina epithelialis (arrows). Nuclear and perinuclear staining of cells of the lamina propria (*) in the mucosa of human ileum as positive control. **d** NOD2 localization in the cytoplasm (arrows) of ccRCC cells. **e** NOD2 is located in cytoplasm primarily in the tubules (arrows and arrowheads). **f** NOD2 localization (arrows) in the mucosa of human ileum as a positive control. **g** Negative staining control of ccRCC and healthy tissue has been performed in the absence of the primary antibodies. **h** Negative staining control of ccRCC and healthy tissue has been performed in the absence of the primary antibodies. **i** Negative staining control of human ileum has been performed in the absence of the primary antibodies. (200 fold magnification)

found in the NOD2 sequence (Supp Fig. 1A) thus corroborating our data.

Constitutive and inducible NOD1 and NOD2 expression in primary isolated tubular epithelial cells of human ccRCC and healthy tissue as well as in CAKI-1 cells

NOD1 and NOD2 was expressed in primary isolated ccRCC cells and tubular epithelial cells (TECs) of healthy renal tissue and displayed higher expression upon incubation with LPS (10 µg/ml) for 4 h. Interestingly, we observed a cluster formation of NOD1 expression upon LPS challenge, which implies, that NOD1 and NOD2 is gradable in human ccRCC and renal tubular epithelial cells. Besides, NOD1 and NOD2 was also constitutively expressed in the human ccRCC cell line CAKI-1.

Shift of NOD1 and NOD2 mRNA expression in a heterotopic tumor model in the mouse

5×10^7 human CAKI-1 cells were injected into nude mice and analyses were performed on tumor homogenates. Messenger RNA expression of both human and mouse NOD1 and NOD2 normalized to the 18 s content were detectable in the tumor tissue, whereby human NOD1 mRNA was significantly higher expressed compared to human NOD2 ($n = 6$, $p < 0.05$) (Fig. 5b), alike in human tumor samples (Fig. 1a). In contrast mouse NOD2 mRNA expression was significantly higher expressed compared to mouse NOD1 ($n = 6$, $p < 0.05$) (Fig. 5b) implying altered human and mouse NOD1 and NOD2 expressions during tumor growth in a heterotopic tumor model. Furthermore, NOD1 and NOD2 receptor expression in CAKI-1 cells was confirmed, displaying also stronger expression of NOD1 than NOD2 (Fig. 6b). In line with higher NOD1 mRNA expression, NOD1 protein

expression was equally higher in immunohistochemically analyzed tumor tissue than NOD2 expression (Fig. 6c).

Discussion

In the present study, we focused on the expression of NOD1 and NOD2 in ccRCC as potential regulator in tumorigenesis. Foremost, according to previous observations from Shigeoka et al. (2010) mRNA expression of NOD1 and NOD2 was detected in healthy renal tissue of all patients. Yet, interestingly, both NOD1 and NOD2 were also detectable in ccRCC tissue. Still, NOD2 mRNA expression was generally markedly lower than NOD1. This fact was previously observed in the mouse prostate tumor model TRAMP (transgenic adenocarcinoma of the mouse prostate) (Kang et al. 2012). Here, NOD1 and NOD2 expressions were detected in the cytoplasm of prostate epithelia, but the intensity of NOD1 was much stronger than that of NOD2 (Kang et al. 2012), which is in line with the observations of the present study. Comparing tumor and healthy renal tissue, the following apportionment stands out: NOD1 mRNA was significantly lower expressed in human tumor tissue compared to adjacent healthy tissue. Inversely, NOD2 mRNA expression was significant higher in human tumor tissue compared to adjacent healthy tissue. These findings are in line with previous in vitro investigations on the human breast cancer epithelial cell line MCF-7 (da Silva Correia et al. 2006), discovering that the absence of NOD1 in human breast cancer cell lines positively correlated with tumor growth due to the absence of NOD1-dependent apoptosis. Conversely, overexpression of NOD1 in MCF-7 cells resulted in inhibition of tumor growth in vitro as well as in a xenograft model of tumor growth in vivo (da Silva Correia et al. 2006). In contrast, NOD2 activation did not induce apoptosis in MCF-7 cells. The statements in this publication correspond to our results regarding the observed lower NOD1 expression in ccRCC tissue. Thus, it is tempting to speculate that the absence of NOD1 in ccRCC could contribute to tumor growth due to the lack of NOD1-dependent apoptosis. This hypothesis is further supported by previous studies showing that NOD1 promoted apoptosis, when overexpressed (Bertin et al. 1999; Inohara et al. 1999). Mechanistically, NOD1 induces the NF-κB pathway via its N-terminal caspase recruitment domain (CARD), a centrally located nucleotide-binding domain (NBD), and a C-terminal regulatory domain (Bertin et al. 1999; Inohara et al. 1999). Confirming results have been achieved by Tukhvatulin et al. (2011) in an comparative in vitro and in vivo study, addressing the ability of NOD1 ligands to activate the transcription factor NF-kB (Tukhvatulin et al. 2011). Upon addition of synthetic NOD1-ligands, a reliable increase in NF-κB could be achieved in vitro. Under in vivo conditions, NOD1-ligand administration resulted in increased NF-κB activation in kidney organ homogenates, albeit to a lesser extent than in other mouse organs. Hence, the observed lower NOD1 mRNA in ccRCC tissue in the present study might be connected to tumor growth due to reduced apoptosis.

However, as individual NOD1 mRNA in tumor tissue correlated strongly with its respective expression in healthy tissue, an inter-individual differing basal expression level of NOD1 may be assumed. This is further supported by the fact that female subjects displayed significantly higher NOD1 mRNA levels in healthy renal tissue compared to male subjects, which equally points to inter-individual differing basal expression levels of NOD1. Nevertheless, opposed to the mRNA expression, NOD1 and NOD2 protein levels in western blot analyses as well as mean fluorescence intensity in flow cytometric analysis of intracellular NOD1 and NOD2 did not significantly alter in tumor tissue nor healthy tissue. This might be explained by post-transcriptional regulation that affects protein translation in ccRCC as this has not been described before with regard to expression of NOD.

Regarding the histomorphological distribution, we noted NOD1 location in the cytoplasm as well as in the nucleus in both ccRCC and healthy tissue. In contrast hereto, NOD2 was solely localized in the cytoplasm. These findings could be validated proving that only NOD1 displays a nuclear localization sequence (NLS) but not the NOD2 sequence. So far, the relevance of NOD1 in both localizations, the nucleus as well as in the cytoplasm, and why it has an NLS still seems unclear.

Given that NOD1 and NOD2 are present in TECs in both mouse and human kidneys (Shigeoka et al. 2010) we first confirmed constitutive NOD1 and NOD2 expression in primary isolated and cultivated TECs of healthy renal tissue, but newly detected also expression in TECs from ccRCC tissue. Interestingly, NOD expression was increasable upon incubation with LPS, applying that both, TECs from tumor or healthy tissue are able to modulate their NOD receptor status upon challenge.

NOD receptors are also known to be constitutively expressed in the human ccRCC cell line CAKI-1 (Uehara et al. 2007). Therefore, we further examined, whether the intracellular sensors NOD1 and NOD2 play also a role in tumor growth in a heterotopic xenograft model in the mouse. Alike to human tumor samples within our patient collective, human NOD1 mRNA was significant higher expressed compared to human NOD2. Though inversely, mouse NOD1 mRNA expression was significantly lower compared to mouse NOD2 mRNA. This applied also for the immunohistochemical detection of NOD1 and NOD2 proteins. As only human CAKI-1 cells have been injected into the mice, mouse mRNA presumably derives from tumor-supporting vascular endothelial cells, which are needed for the onset of tumor-supporting neo-vascularization (Folkman et al.

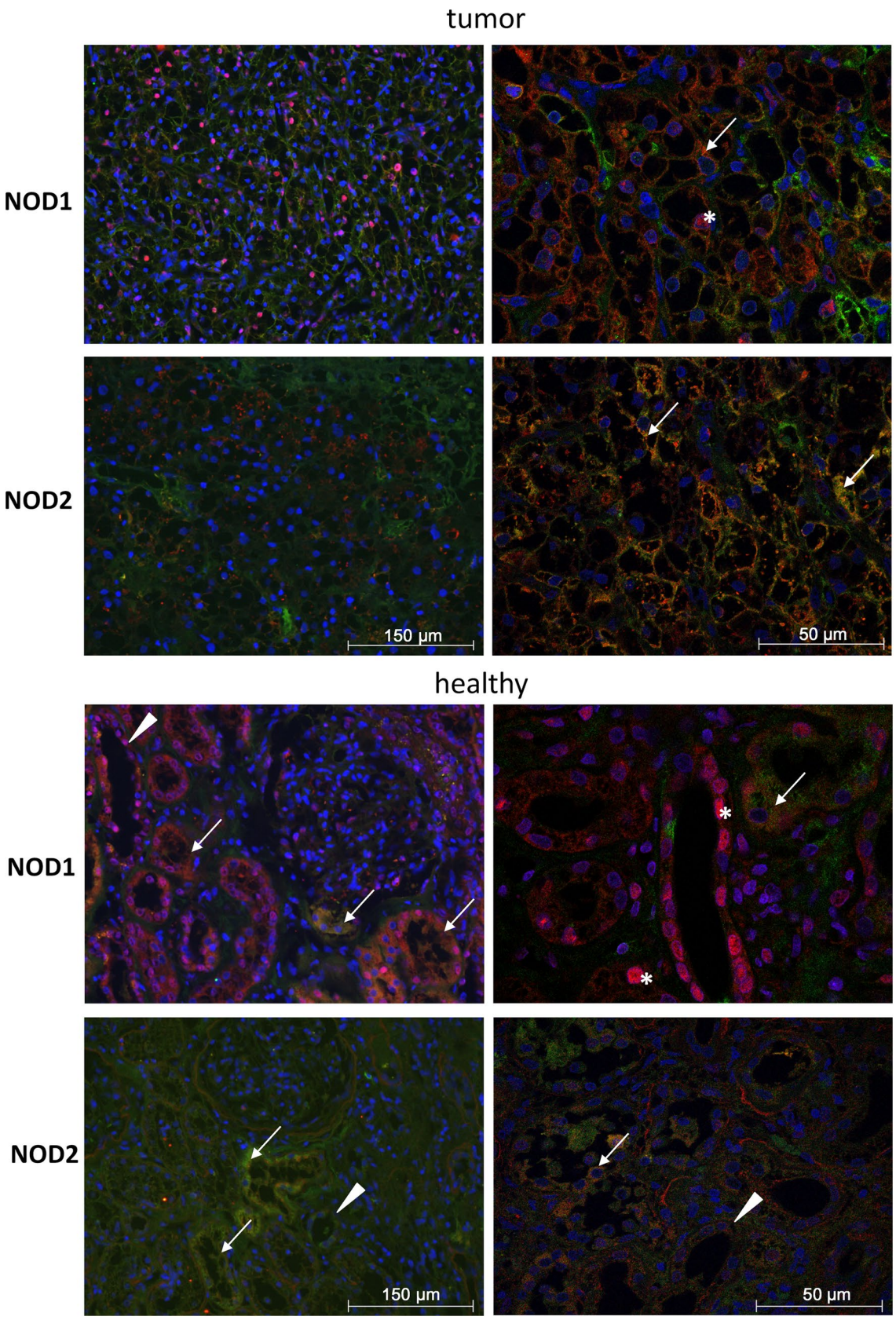
tumor
NOD1
NOD2
150 µm
50 µm
healthy
NOD1
NOD2
150 µm
50 µm

◂**Fig. 3** Immunofluorescence staining of NOD1 and NOD2 receptor in ccRCC and healthy tissue. Immunofluorescence staining of NOD1 and NOD2 receptor in red (Cy3) and proximal tubule specific CD13 in green (Alexa 488) in ccRCC and healthy renal tissue. Co-localization appear as merge in yellow. Nuclear staining was performed using DAPI. Assessment with confocal microscopy (right pictures). Nuclear (white*) and cytoplasmic (white arrows and arrowheads) localization of NOD1 and NOD2 receptor. Higher expression of NOD1 receptor in healthy kidney, especially in proximal (white arrows), distal (white arrowheads) and collecting duct. Co-localization of NOD1 with CD13 in the proximal tubuli (white arrows). High NOD2 expression occurs in tumor tissue (left pictures in 200-fold and right pictures in 600-fold magnification)

1989). Referring to this, expression of NOD1 and NOD2 in human (Oh et al. 2005; Opitz et al. 2005; Davey et al. 2006) and murine (Scurrell et al. 2009) endothelial cells has been shown previously. Hence, we had a closer look at the vasculature within our human tissue samples and we detected markedly more pronounced NOD2 than NOD1 expression within vascular endothelial cells especially in renal tumor tissue showing vivid angiogenesis. Although no altered vascular permeability has been observed in NOD1/2 deficient mice during renal ischemia reperfusion injury (Stroo et al. 2012), the possibility of other regulatory pathways, like activation of pro-angiogenic factors (Schirbel et al. 2013) resulting in endothelial growth is conceivable.

Particularly, considering that therapeutic targeting of VEGF in RCC, and herewith vasculature, has a strong biologic rationale (Rini 2005), one could hypothesize that NOD receptors also exert a relevant effect. Succinctly, lower apoptosis-associated NOD1 expression in ccRCC tissue with opposed hereto high expression of NOD2 in tumor vasculature, inducibility of NOD expression in TECs as well as the observed shift of NOD1 and NOD2 expression in the mouse xenograft model might point to their different path of influencing carcinogenesis as also suggested previously (da Silva Correia et al. 2006).

The present study contributes to a better understanding of the complex relationship between ccRCC, its vasculature and NOD1 as well as NOD2 of the innate immunity. Since targeted- and immuno-therapy plays a central role in the

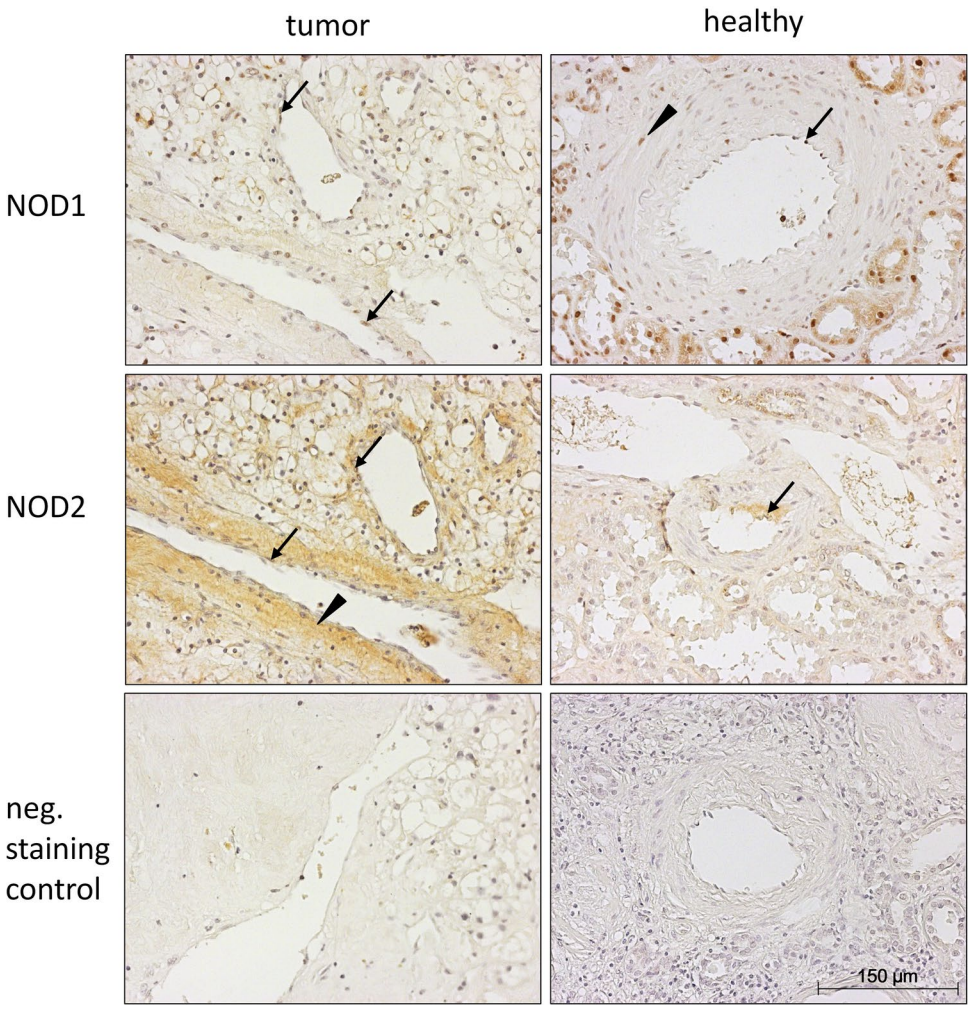

Fig. 4 Immunohistochemical staining for NOD1 and NOD2 receptors in ccRCC and healthy tissue vasculature. Localization of NOD1 or NOD2 in endothelial cells (arrows) and tunica media (arrowhead). Negative staining control of ccRCC and healthy tissue has been performed in the absence of the primary antibodies. (200 fold magnification)

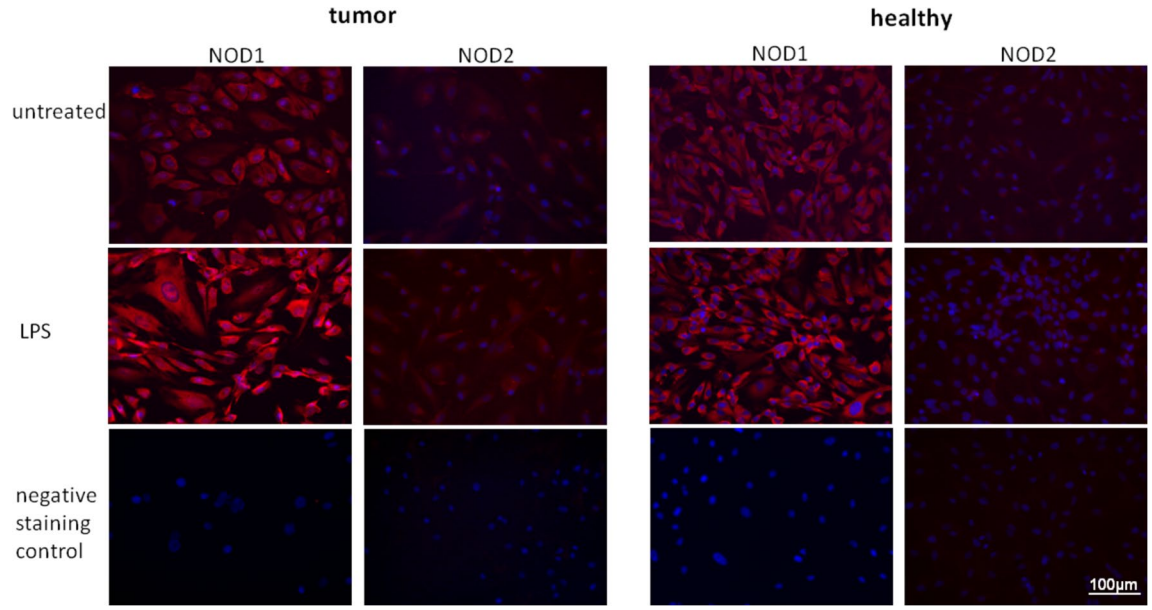

Fig. 5 Immunofluorescence staining of NOD1 and NOD2 receptor in primary isolated ccRCC cells and corresponding renal tubular epithelial cells (TECs). NOD1 and NOD2 expression in red (Cy3) in primary isolated tumor cells and renal tubular epithelial cells (TECs) of healthy tissue. TECs were untreated or incubated with LPS (10 µg/ml) for 4 h. Nuclear DAPI staining. Negative staining control was performed without the use of primary antibody. (200-fold magnification)

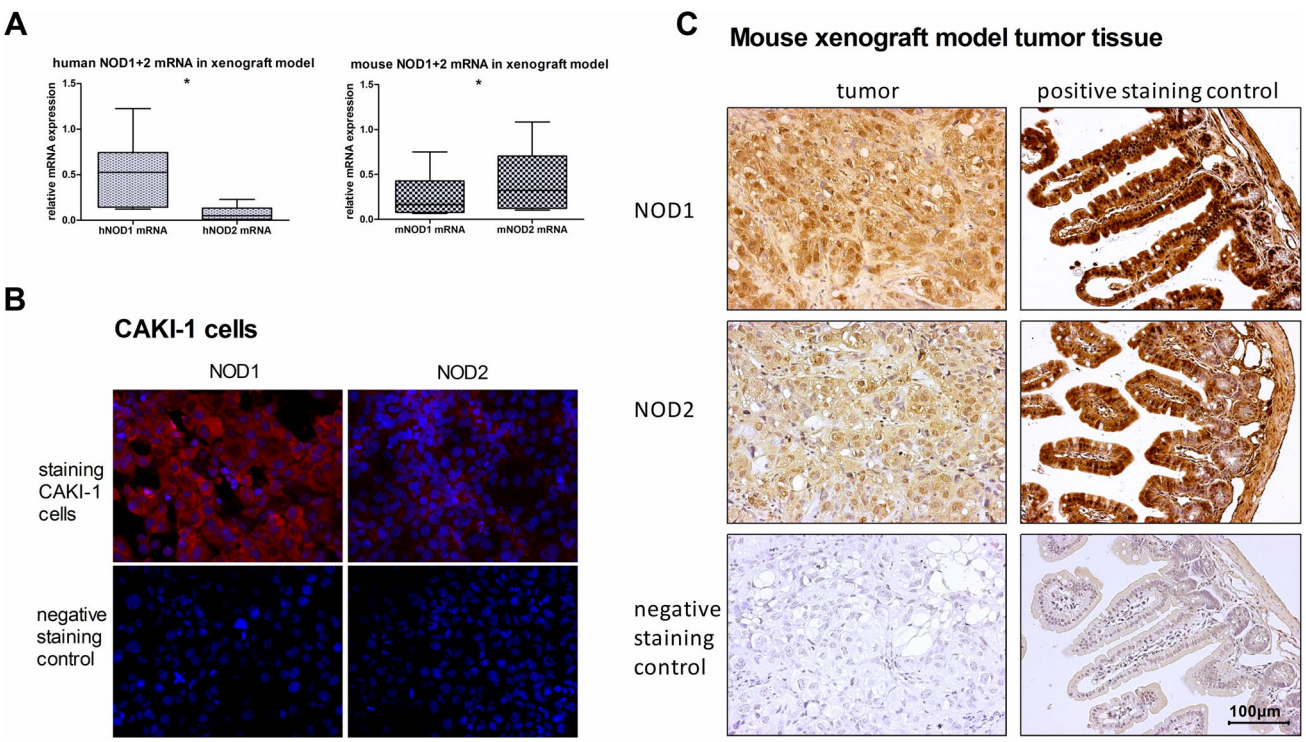

Fig. 6 NOD1 and NOD2 expression in a heterotopic tumor model in the mouse. **a** Human NOD1 and NOD2 mRNA as well as mouse NOD1 and NOD2 mRNA expression normalized to its 18 s content in a heterotopic tumor model in the mouse ($n=6$) presented in box blots to depict the distributions of the relative expression values. *$p<0.5$. **b** Immunofluorescence staining of NOD1 and NOD2 receptor in CAKI-1 cells. NOD1 and NOD2 expression in red (Cy3) in untreated CAKI-1 cells. Nuclear DAPI staining. Negative staining control was performed without the use of primary antibody (200-fold magnification). **c** Immunohistochemical staining of NOD1 and NOD2 receptor in tumor areas of the xenograft model and mouse ileum as positive control. Negative staining control was performed without the use of primary antibody (200-fold magnification)

therapy of advanced renal cell carcinoma, this study may contribute to new therapeutic approaches.

Acknowledgements We especially thank Svenja Stumpf, Melanie Berger and Michael Dreher for their technical support. The study was financed by a grant from the Kulemann-Stiftung, Germany to AU. The foundation had no influence on design of the study, data collection and interpretation or on the decision to publish.

Compliance with ethical standards

Conflict of interest The authors declare that they have no conflict of interest and that the results presented in this paper have not been published previously in whole or part.

Ethical approval All procedures performed in studies involving human participants were in accordance with the ethical standards of the institutional and/or national research committee and with the 1964 Helsinki declaration and its later amendments or comparable ethical standards. All procedures performed in studies involving animals were in accordance with the ethical standards of the institution or practice at which the studies were conducted.

References

Baer PC, Nockher WA, Haase W, Scherberich JE (1997) Isolation of proximal and distal tubule cells from human kidney by immunomagnetic separation. Kidney Int 52:1321–1331

Bamias A et al (2017) Current clinical practice guidelines for the treatment of renal cell carcinoma: a systematic review and critical evaluation. Oncologist 22:667–679. https://doi.org/10.1634/theoncologist.2016-0435

Bertin J et al (1999) Human CARD4 protein is a novel CED-4/Apaf-1 cell death family member that activates NF-kappaB. J Biol Chem 274:12955–12958

Braunstein MJ, Kucharczyk J, Adams S (2018) Targeting toll-like receptors for cancer therapy. Target Oncol. https://doi.org/10.1007/s11523-018-0589-7

Bray F, Ferlay J, Soerjomataram I, Siegel RL, Torre LA, Jemal A (2018) Global cancer statistics 2018: GLOBOCAN estimates of incidence and mortality worldwide for 36 cancers in 185 countries. Cancer J Clin. https://doi.org/10.3322/caac.21492

Caruso R, Warner N, Inohara N, Nunez G (2014) NOD1 and NOD2: signaling, host defense and inflammatory disease. Immunity 41:898–908. https://doi.org/10.1016/j.immuni.2014.12.010

da Silva Correia J et al (2006) Nod1-dependent control of tumor growth. Proc Natl Acad Sci USA 103:1840–1845. https://doi.org/10.1073/pnas.0509228103

Davey MP, Martin TM, Planck SR, Lee J, Zamora D, Rosenbaum JT (2006) Human endothelial cells express NOD2/CARD15 and increase IL-6 secretion in response to muramyl dipeptide. Microvasc Res 71:103–107. https://doi.org/10.1016/j.mvr.2005.11.010

Folkman J, Watson K, Ingber D, Hanahan D (1989) Induction of angiogenesis during the transition from hyperplasia to neoplasia. Nature 339:58–61. https://doi.org/10.1038/339058a0

Hisamatsu T, Suzuki M, Reinecker HC, Nadeau WJ, McCormick BA, Podolsky DK (2003) CARD15/NOD2 functions as an antibacterial factor in human intestinal epithelial cells. Gastroenterology 124:993–1000. https://doi.org/10.1053/gast.2003.50153

Inohara N et al (1999) Nod1, an Apaf-1-like activator of caspase-9 and nuclear factor-kappaB. J Biol Chem 274:14560–14567

Inohara N, Ogura Y, Chen FF, Muto A, Nunez G (2001) Human Nod1 confers responsiveness to bacterial lipopolysaccharides. J Biol Chem 276:2551–2554. https://doi.org/10.1074/jbc.M009728200

Kang MJ et al (2012) Activation of Nod1 and Nod2 induces innate immune responses of prostate epithelial cells. Prostate 72:1351–1358. https://doi.org/10.1002/pros.22483

Koebel CM et al (2007) Adaptive immunity maintains occult cancer in an equilibrium state. Nature 450:903–907. https://doi.org/10.1038/nature06309

Kosugi S, Hasebe M, Tomita M, Yanagawa H (2009) Systematic identification of cell cycle-dependent yeast nucleocytoplasmic shuttling proteins by prediction of composite motifs. Proc Natl Acad Sci USA 106:10171–10176. https://doi.org/10.1073/pnas.0900604106

Livak KJ, Schmittgen TD (2001) Analysis of relative gene expression data using real-time quantitative PCR and the 2(-Delta Delta C(T)) method. Methods 25:402–408. https://doi.org/10.1006/meth.2001.1262

Ogura Y, Inohara N, Benito A, Chen FF, Yamaoka S, Nunez G (2001) Nod2, a Nod1/Apaf-1 family member that is restricted to monocytes and activates NF-kappaB. J Biol Chem 276:4812–4818. https://doi.org/10.1074/jbc.M008072200

Ogura Y et al (2003) Expression of NOD2 in Paneth cells: a possible link to Crohn's ileitis. Gut 52:1591–1597

Oh HM et al (2005) Induction and localization of NOD2 protein in human endothelial cells. Cell Immunol 237:37–44. https://doi.org/10.1016/j.cellimm.2005.09.006

Opitz B et al (2005) Nod1-mediated endothelial cell activation by *Chlamydophila pneumoniae*. Circ Res 96:319–326. https://doi.org/10.1161/01.RES.0000155721.83594.2c

Park JH et al (2007) Nod1/RICK and TLR signaling regulate chemokine and antimicrobial innate immune responses in mesothelial cells. J Immunol 179:514–521

Parlato M, Yeretssian G (2014) NOD-like receptors in intestinal homeostasis and epithelial tissue repair. Int J Mol Sci 15:9594–9627. https://doi.org/10.3390/ijms15069594

Patard JJ et al (2005) Prognostic value of histologic subtypes in renal cell carcinoma: a multicenter experience. J Clin Oncol 23:2763–2771. https://doi.org/10.1200/JCO.2005.07.055

Rini BI (2005) VEGF-targeted therapy in metastatic renal cell carcinoma. Oncologist 10:191–197. https://doi.org/10.1634/theoncologist.10-3-191

Schirbel A et al (2013) Pro-angiogenic activity of TLRs and NLRs: a novel link between gut microbiota and intestinal angiogenesis. Gastroenterology 144:613–623 e619. https://doi.org/10.1053/j.gastro.2012.11.005

Scurrell E, Stanley R, Schoniger S (2009) Immunohistochemical detection of NOD1 and NOD2 in the healthy murine and canine eye. Vet Ophthalmol 12:269–275 https://doi.org/10.1111/j.1463-5224.2009.00698.x

Shigeoka AA et al (2010) Nod1 and nod2 are expressed in human and murine renal tubular epithelial cells and participate in renal ischemia reperfusion injury. J Immunol 184:2297–2304. https://doi.org/10.4049/jimmunol.0903065

Stroo I et al (2012) Phenotyping of Nod1/2 double deficient mice and characterization of Nod1/2 in systemic inflammation and associated renal disease. Biol Open 1:1239–1247 https://doi.org/10.1242/bio.2012554

Thoenes W, Storkel S, Rumpelt HJ (1986) Histopathology and classification of renal cell tumors (adenomas, oncocytomas and carcinomas). The basic cytological and histopathological elements and their use for diagnostics. Pathol Res Pract 181:125–143. https://doi.org/10.1016/S0344-0338(86)80001-2

Ting JP, Davis BK (2005) CATERPILLER: a novel gene family important in immunity, cell death and diseases. Annu Rev Immunol 23:387–414. https://doi.org/10.1146/annurev.immunol.23.021704.115616

Tukhvatulin AI et al (2011) A in vitro and in vivo study of the ability of NOD1 Ligands to activate the transcriptional factor NF-kB. Acta Naturae 3:77–84

Uehara A, Fujimoto Y, Fukase K, Takada H (2007) Various human epithelial cells express functional Toll-like receptors, NOD1 and NOD2 to produce anti-microbial peptides but not proinflammatory cytokines Mol Immunol 44:3100–3111. https://doi.org/10.1016/j.molimm.2007.02.007